Hindawi

Research Article

Deformation Characteristics and Safety Evaluation of the Throw Filling Soft Clay Cofferdam under Super-Historical Flood Conditions

Ping Jiang,[1] **Yong Huang,**[2] **Zhipeng Tao,**[3] **Junhua Zhu** (ORCID),**[4,5,6] **Ning Wang,**[5] **and Jianwei Qiao**[7]

[1]*Jiangxi Port Group Co., Ltd., Nanchang 330062, China*
[2]*Jiangxi Road and Port Engineering Co., Ltd., Nanchang 330062, China*
[3]*Jiangxi Transportation Institute Co., Ltd., Nanchang 330062, China*
[4]*School of Civil Engineering and Architecture, East China Jiaotong University, Nanchang 330013, China*
[5]*State Key Laboratory of Performance Monitoring Protecting of Rail Transit Infrastructure, East China Jiaotong University, Nanchang 330013, China*
[6]*Engineering Research & Development Centre for Underground Technology of Jiangxi Province, Nanchang 330013, China*
[7]*China Jikan Research Institute of Engineering Investigations and Design Co., Ltd., Xi'an 710043, China*

Correspondence should be addressed to Junhua Zhu; 3062@ecjtu.edu.cn

Affected by super-historical flood, the surface deformation of throw filling soft clay cofferdam is obvious and the stability of the cofferdam slope is difficult to ensure. Relying on the cofferdam project of Jiangxi Xinjiang Shuanggang navigation power junction and according to the data of filed investigation and automatic monitoring, the Plaxis infinite element software is used to analyze the deformation characteristics and stabilities of cofferdam during the super-historical flood period, and the effective emergency reinforcement measures are presented. The results show that (1) the stability of cofferdam is controlled by downstream face slope of cofferdam during the super-historical flood period, and there is a most dangerous slide surface interpenetrating through the top to the toe of downstream face slope; (2) the stability of upstream face slope is influenced significantly by the water level fluctuation and it is reduced sharply during the water level decline process; and (3) real-time remote monitoring can effectively reflect the deformation and failure characteristics of cofferdam under the condition of super-historical flood level and provide early warning and prediction in time. The results and analyzing methods can be applied to analyze the similar projects excellently.

1. Introduction

In hydropower and navigation junction projects, the cofferdam is designed according to the diversion flow of design frequency and corresponding water level to carry out construction diversion and ensure the continuous construction of main works [1–5]. At the same time, the year-round cofferdam as a temporary water-blocking building during the river flood season, its stability in flood period is an important premise to protect the construction personnel in the weir and the safety of the project [6, 7].

In the diversion system of earth rock cofferdam, slope instability is not only the most frequent but also the most loss and the most difficult to make up [8–12]. In addition to the stability of the cofferdam under the action of self weight, the seepage will also lead to the instability of the cofferdam body under the condition of water level difference inside and outside the cofferdam [13–17]. During the flood period, the rise of water level leads to the increase in soil moisture content and the decrease in shear strength, and the pore water pressure in the slope is also in dynamic change with the rise and fall of water level [18, 19]. At the same time, the stress condition and antisliding ability of cofferdam slope will be changed by flood pressure and immersion [20]. In the study by Zhang [21], according to the deformation mechanism of some landslides after the change of water level in

the Three Gorges reservoir, from the analysis, the rise of reservoir water level has limited influence on landslide deformation, but the decline of water level will directly lead to landslide. Luo [22] through integrating on-site investigation, monitoring data, and numerical simulation, the formation mechanism and deformation characteristics of Waitang landslide are revealed, in which rainfall and reservoir water level change are the main factors affecting slope behavior; Xiao et al. [23], using the method of intermittent decline of reservoir water level to trigger landslide, studied the effect of rapid change of water level on landslide stability; the analysis shows that the intermittent drop is beneficial to the dissipation of hole pressure in the landslide body, but when the reservoir water level decreases too fast, there is a lag effect of groundwater fall back beneficial to the reduction of hydraulic gradient.

In the study by Wang et al. [24], through the comparison and analysis of the stability of different processes of flood rise, flood immersion, and flood decline, it is pointed out that the stability of the shore beach is the best during the period of rapid flood rise, followed by the period of slow rise, soak period, and slow decline of flood, and the stability of shore beach is the worst during the period of flood plunge.

From the existing research, most of them are aimed at the deformation characteristics and instability mechanism of earth rock cofferdam, clay core dam, and reservoir bank slope under the condition of water level fluctuation or flood, while there are few studies on soft clay cofferdam formed by the throw filling [25–30]. Due to the shortage of filling materials, the cofferdam of Shuanggang navigation power junction project in Xinjiang, Jiangxi Province, mainly adopted silty clay excavated by diversion channel with low shear strength, low bearing capacity, and high water content and supplemented by outsourcing soil. In the cofferdam operation stage in July 2020, with the water level outside the cofferdam raised to 20.8 m that exceeded the design flood water level, there is certain deformation in the surface of the cofferdam and posed a great threat to the stability of it. This paper lies on this project; according to the data of filed investigation and automatic monitoring, the finite element software named Plaxis is applied to analyze the deformation characteristics and evaluate the safety situation of cofferdam during the super-historical period, presenting the emergency reinforcement measures to provide reference for the similar projects.

2. Background of Project

2.1. General Situation of Cofferdam.
The main construction of Jiangxi Xinjiang Shuanggang navigation power junction project is located in the distance of 5 km far away from downstream of Poyang Town, Shangrao City. For providing the drying construction condition for building main structures, a cofferdam should be fabricated. Due to the shortage of filling materials, the perennial cofferdam filling is mainly filled with saturated silty clay mixed with muddy soil from the riverbed excavated by diversion channel, and some outsourcing soil is purchased for the backfilling of the cofferdam dike core to strengthen the cofferdam and form roads. The total length of the cofferdam is 2454 m, including 450 m length of upstream cofferdam, 1459 m length of longitudinal cofferdam, and 545 m length of downstream cofferdam, with the service life of the cofferdam which belongs to the perennial cofferdams ranging from 2 to 2.5 years. According to the Design Code for Cofferdams of Water Resources and Hydropower Engineering (SL645-2013), the lock level is Class II and the design level of the cofferdam is Class IV. The layout of diversion channel and cofferdam is shown in Figure 1.

The design of lowest water level and flood water level is 13.92 m and 19.94 m. The molding of throw filling soft clay cofferdam is really hard because of the high compressibility and low strength of filling materials. After the stable molding, the actual shape of the cofferdam is different from the design shape that the actual slope ratios of the cofferdam above the horse path whose elevation is 14 m at both of upstream and downstream cofferdam are less than 1 : 5, and the slope ratio of the slope whose elevation is lower than 14 m is less than 1 : 7, and it is more gentle at the center location where the slope ratio is 1 : 31 eventually.

2.2. Automatic Monitoring of Cofferdam.
Considering the lack of experience references for this type of cofferdam and because of the low strength, discreteness of mechanical properties, and uncertainties of spatial distribution of filling materials, the automatic monitoring of displacement and seepage force is applied to monitor the real-time deformation and stability of the cofferdam for ensuring the safety operation of it. The arrangement plan of automatic monitoring is shown in Figure 2. According to the results of numerical simulation and field experience, the early warning value and alarm value of horizontal displacement rate of the cofferdam is set as 1.5 mm/d and 2.0 mm/d [31, 32].

2.3. General Situation of Super-Historical Flood.
In July 2020, affected by the superposition of continuous heavy rainfall and upstream river water, the water level of Xingzi station which is a landmark hydrological station of Poyang Lake was raised to 22.53 m that it was 0.01 m higher than the historical highest water level of 22.52 m in 1998; the water level of Poyang Lake broke through the historical extreme value since the exist of hydrological record.

Affected by the super-historical flood, the water level outside the cofferdam is reached to 20.8 m that it is 0.86 m higher than the design flood water level of the cofferdam. From June 30 to July 12, the increment of water level outside the cofferdam was 4.91 m, and the maximum water level increasing rate was 0.81 m/d, which was higher than the maximum daily water level increasing rate in 1998. The change curve of water level outside the cofferdam during flood period is shown in Figure 3.

3. Analysis on Deformation Characteristics of Cofferdam in Flood Period

The field investigation shows that under the action of super-historical flood, the cofferdam slope has certain deformation and damage, which is mainly concentrated in the upstream

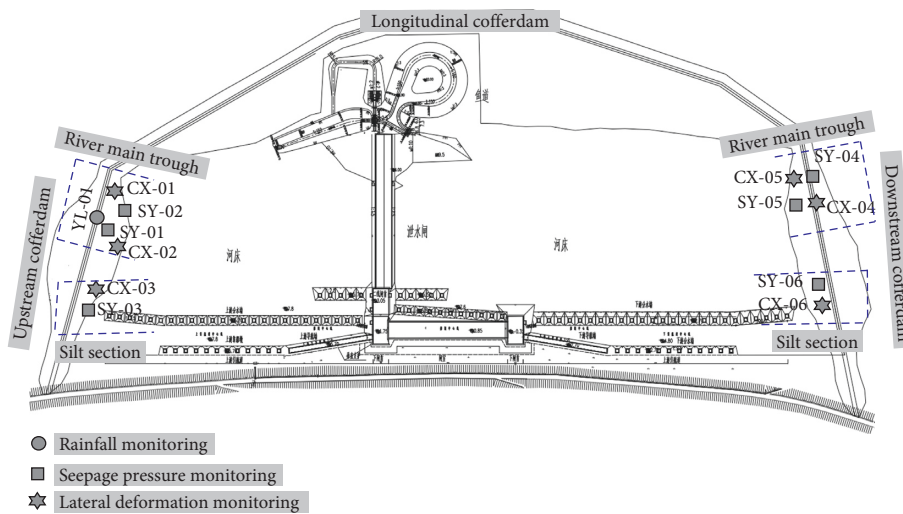Figure 1: Layout of cofferdam and divert.

Figure 2: Schematic layout of cofferdam slope monitoring points.

cofferdam. According to the data of field investigation and automatic monitoring, the deformation characteristics of cofferdam during the flood rising period and flood decline period are analyzed in this paper.

3.1. Deformation Characteristics of Cofferdam in Flood Rising Period.

According to the field investigation, in the flood rising period, the deformation and damage area are located in the riverbed center of upstream cofferdam where the thickness of filling material is maximum. Because the height difference between the flood water level and the top of cofferdam is just 0.2 m, a surcharge load of sand bags whose height and width are 1 m and 2 m is carried out at the upstream side of cofferdam for preventing the cofferdam exceeded by the flood water. However, influenced by the surcharge load, a tensile fissure and meteorism deformation

occurred at the top of cofferdam. The length and width of the tensile fissure are 99 m and 2.0~3.0 cm separately as shown in Figure 4 and the strike almost parallels with the extended direction of road. The height of meteorism deformation is 6.0~8.0 cm generally.

Meanwhile, there is a small sized piping damage occurred at the position of elevation of 11 m which is located in the horse path of downstream face caused by the huge seepage force which is formed by the water head difference between upstream face and downstream face. Fortunately, the filling material of cofferdam almost consists of clay particles whose permeability is small so that the seepage water from the piping is clean and there is a small threat to the stability of cofferdam (as shown in Figure 5).

According to the distribution of deformation area, the real-time monitoring data of measuring points cx-01, cx-02, and sw-01 are selected to comparative analysis. The results
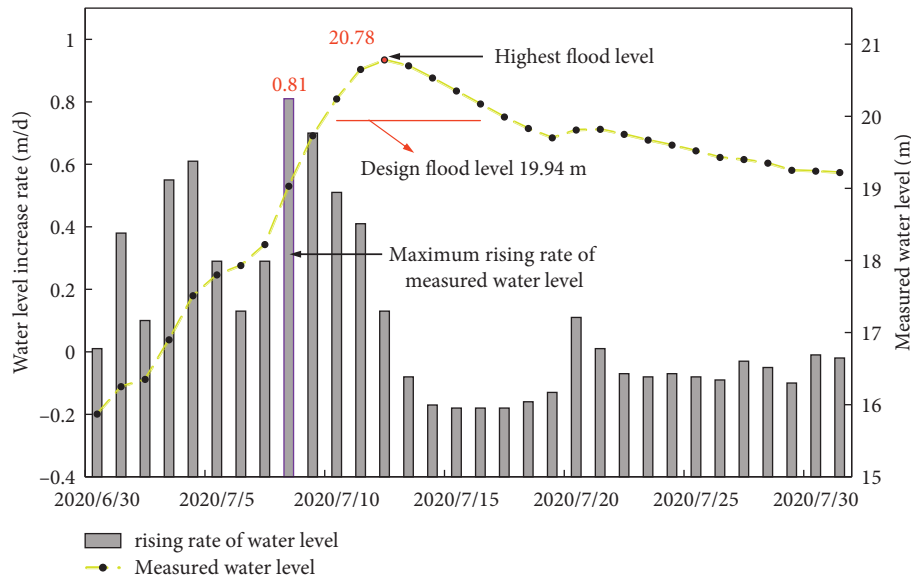
FIGURE 3: Curve of water level change outside the cofferdam during flooding.

FIGURE 4: Tensile fissure at the top of upstream cofferdam.

FIGURE 5: Piping effect at downstream face slope of cofferdam.

show that (Figure 6), during the flood rising period, the soil deformation rate below the path way is small and the state is stable. However, the soil above the path way of the downstream face has an accelerated deformation rate, and the maximum value reaches to 1.95 mm/d that is closing to the alarm value, and there is a potential risk of sliding. The generation and development of tensile cracks are closely related to the displacement of the soil below the cofferdam crest of the downstream face slope.

The growth rate of the water level in the cofferdam lags behind the growth rate of outside water level during the super-historical flood raising period. The high head difference between the flood water level (20.78 m) and the water level in the cofferdam (11 m) is an important reason for the local piping failure. Considering the risk of instability and damage of cofferdam, the emergency treatment measures shall be taken to reinforce the cofferdam as follows: concrete grouting reinforcement is carried out in the tensile fissure area; the height of piping well is increased and the geotextile is laid aside the piping outlet; a flood spillway is set to reduce the water head difference between outside and inside of the cofferdam.

3.2. Deformation Characteristics of Cofferdam in Flood Decline Period. The tensile fissure and meteorism deformation which has been reinforced at the top of cofferdam continue to develop that the width of tensile fissure is increased to 4 cm and the height of meteorism deformation is increased to 10 cm (Figure 7). The scope of piping is not expanding, and its flow rate is reduced benefitting from the reinforcement measure.

The real-time monitoring results show (Figure 6) that the deformation rate of potential sliding area is less than 1.5 mm/d and the situation of deformation rates is
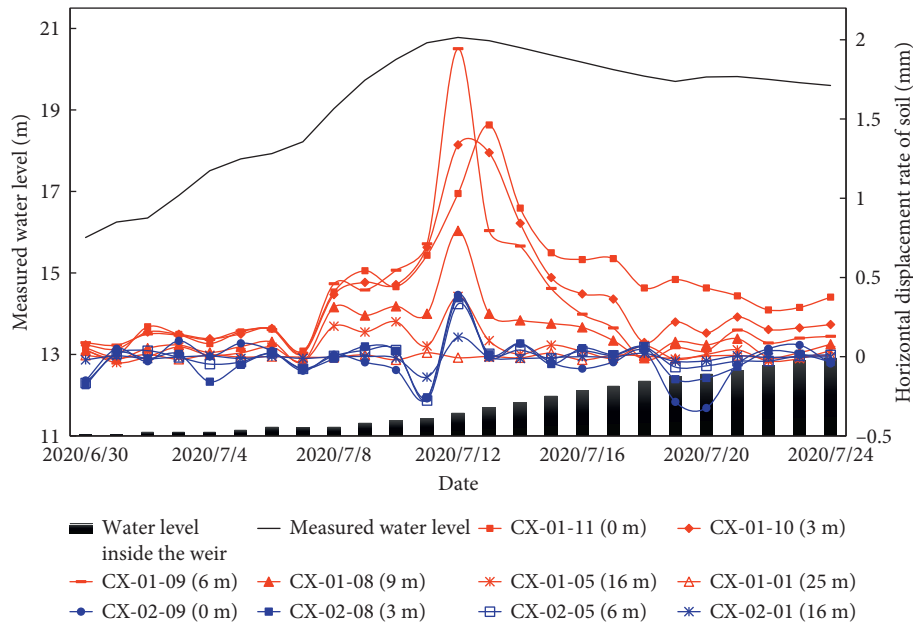
FIGURE 6: The displacement changing rates of CX-01 and CX-02 during the super-historical flooding period.
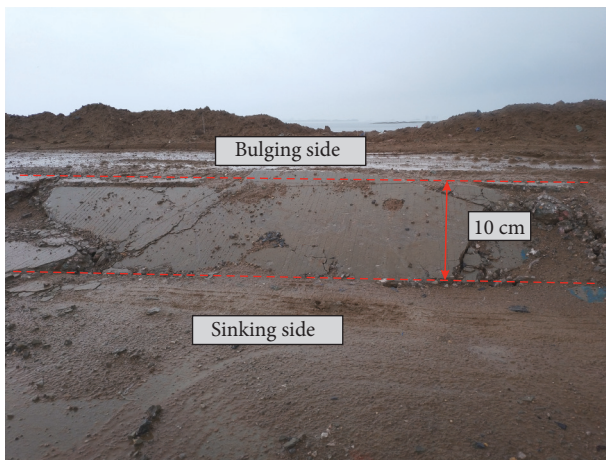

FIGURE 7: Meteorism deformation in the top of upstream cofferdam during flood decline period.

convergent during the super-historical flood decline process. It demonstrates that the emergency reinforcement measurements are effective and the cofferdam tides over the super-historical period safely. Due to the influence of upstream face head pressure and cofferdam foundation drainage, the water level inside the cofferdam gradually rises, and the water level difference inside and outside of the cofferdam is reduced, avoiding the development of piping damage.

4. Stability Evaluation of Cofferdam Slope and Discussion

As mentioned above, the dynamic change of outside flood water level will not only affect the development of cofferdam slope but also change the seepage state of soil inside the cofferdam, resulting in the increase in soil moisture content and the decrease in shear strength. In addition, influenced by the water head difference between outside and inside of cofferdam, the stability of the cofferdam slope will be reduced caused by the seepage force inside the cofferdam (see Zhang and Hu [33]). For further research and verification, the finite element numerical software named Plaxis is used to analyze the stability state of the cofferdam during the super-historical flood period [34].

4.1. Computational Model. According to the field investigation and drilling boring information, a 2-dimensional calculation model is established by the Plaxis software, which represents the most dangerous profile of the cofferdam as shown in Figure 8.

4.2. Computing Method. Mohr–Coulomb model is selected to describe the constitutive model of filling materials, and liner-elastic model is selected to describe the impermeable wall [35]. It is assumed that the flow of pore water accords with Darcy's law, and the coupling effect of seepage field and stress field during the water level fluctuation is considered in the seepage analysis process. Furthermore, a shear strength reduction factor ΣMSF leads to the calculation of stability of the cofferdam that making the strength parameter C and φ and the tensile strength decrease gradually until the soil is damaged [36]. The ΣMSF is defined as follows:

$$\sum M_{sf} = \frac{\tan \phi_{\text{input}}}{\tan \phi_{\text{reduced}}} = \frac{c_{\text{input}}}{c_{\text{reduced}}}. \tag{1}$$

In the formula, ϕ_{input} is the internal friction angle of soil mass; c_{input} is the initial cohesion; ϕ_{reduced} is the internal friction angle of soil mass after the strength
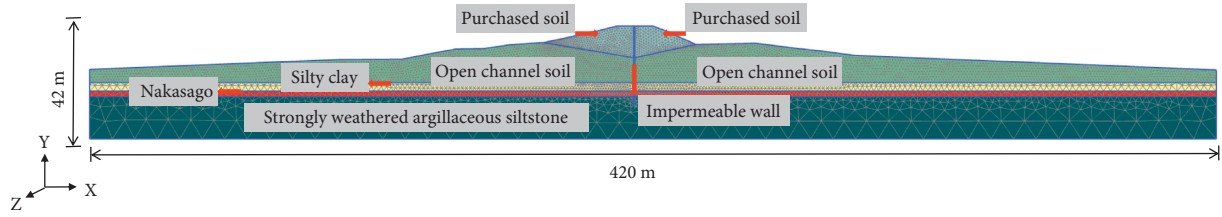
Figure 8: Cofferdam structure and filling distribution.

Table 1: Properties of soils/rocks of the cofferdam and foundation.

Cofferdam material	Cohesion (kPa)	Internal friction angle (°)	Permeability coefficient (cm·s^{-1})	Natural bulk density (kN·m^{-3})	Saturated bulk density (kN·m^{-3})	Elastic modulus (kPa)	Poisson's ratio	Thickness (m)
Outsourcing soil	34.1	13.4	6.17×10^{-5}	18.40	19.30	11260	0.30*	6.0~8.0
Outsourcing soil soaked in flood (upstream face)	30.1	13.4	6.17×10^{-5}	18.40	19.30	11260	0.30*	6.0~8.0
Open channel backfill (upstream face)	19.0	9.0	6.17×10^{-5}	18.00	18.30	10580	0.35*	13.0~15.0
Open channel backfill (downstream face)	12.5	7.0	6.17×10^{-5}	18.00	18.30	10580	0.35*	13.0~15.0
Silty clay	20.0	13.0	7.0×10^{-5}	18.80	20.00	8840*	0.30*	1.5
Medium sand	0.0	28.0	1.0×10^{-3}	18.00	19.00	12000*	0.30*	0.5
Strongly weathered argillaceous siltstone	100.0	35.0	1.0×10^{-4}	20.00	21.00	300000*	0.30*	—
Impermeable wall	—	—	5.0×10^{-6}	22.00	23.00	300000*	0.20*	—

reduction; and c_{reduced} is the cohesion after the strength reduction.

Assume that if the calculation model does not converge during the numerical analysis, it indicates that the cofferdam or its foundation reaches completely destruction, and the corresponding safety factor is as follows:

$$SF = \frac{\text{usablestrength}}{\text{failurestrength}} = \sum M_{sf} = (\text{atfailure}). \qquad (2)$$

According to 《Design code for cofferdam of water resources and hydropower engineering》 (SL645-2013), when the design level of cofferdam is IV, the safety factor of antisliding stability of cofferdam slope is $k \geq 1.05$.

4.3. Parameter Selection. The silty clay and outsourcing soils disturbed by both excavation and throw filling are filled as the main structure of the cofferdam, causing the huge discreteness on the physical and mechanical parameters of the filling materials that are hard to determine. Therefore, an antianalysis method is applied to analyze the mechanical parameters of the filling materials in different conditions based on the data of automatic monitoring, laboratory tests, and experience. As the length limitation of this paper, the specific analysis process would not be mentioned. The final physical and mechanical parameters of rock and soil are shown in Table 1.

4.4. Calculating Conditions. Combined with the water level monitoring data outside the cofferdam and considering the flood change time history, the measured water level from March 24 to November 1, 2020, is selected to simulate the whole process of flood operation situation of the cofferdam in flood season and analyze the change of cofferdam slope stability coefficient under the change of water level. Calculation working conditions include stable operation stage of cofferdam before flood (working condition $A1$), flood rising stage (working condition $B2$), pile-loading sandbags on weir crest at upstream side, stable seepage stage of flood level (working condition $C3$), and flood falling stage (working condition $D4$), as shown in Table 2.

4.5. Calculation Results Analysis and Discussion. The cofferdam stability safety factor obtained under all the above working conditions is listed in Table 3; it indicates that

(1) The safety factors of cofferdam are greater than 1.05 entirely during the whole process of super-historical flood season, and the overall stability of cofferdam is controlled by the downstream face slope, and the condition of flood water decline is the most unfavorable working condition, and the minimum safety factor is 1.58 in $D4$ condition. The cofferdam is in a stable state.

TABLE 2: Load combinations for cofferdam stability analysis.

Calculation conditions	Illustrate	Measured water level outside of the cofferdam	Cofferdam top loading
A1	Stable operation of the cofferdam before the flood	March 24–June 30, 2020	—
B2	Flood rising period	July 01–July 11, 2020	—
C3	Loaded sand bags, stable seepage at flood level (20.78 m)	July 12, 2020	20 kN/m^2
D4	Flood decline period	July 12–November 1, 2020	20 kN/m^2

TABLE 3: Factor of safety (FOS) of cofferdam stability for all load conditions.

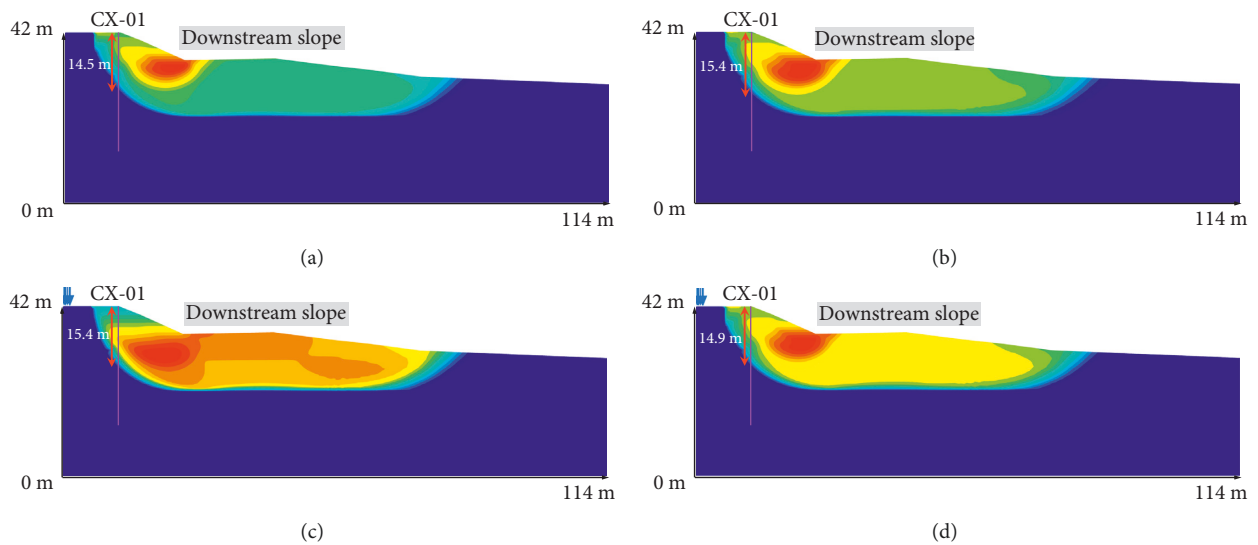| Calculation working condition	Upstream face side slope Minimum safety factor	Downstream face side slope Minimum safety factor	Entirety cofferdam Minimum safety factor	Destabilization side
A1	2.04	1.64	1.65	Downstream face
B2	3.12	1.60	1.61	Downstream face
C3	2.92	1.62	1.62	Downstream face
D4	1.94	1.57	1.58	Downstream face

FIGURE 9: Horizontal displacement clouds of the backwater slope hazardous slip surface: (a) working condition A1; (b) working condition B2; (c) working condition C3; (d) working condition D4.

(2) The change of water level significantly affects the stability of the upstream face slope, and the stability safety factor decimated in the process of flood declines that the reduction rate of safety factor between the maximum and minimum value is 37.8%.

(3) During the whole process, the surcharge load at the top of cofferdam has a positive effect to the stability of whole cofferdam, but it will reduce the stability of upstream face slope and the reduction rate is 6.4%. Therefore, we suggest that the surcharge load of sand bags should be loaded at the axis of the top of the cofferdam.

(4) As shown in Figure 9, the minimum safety factors of actual slope types in all conditions are located in the downstream face entirely, and the displacement value and the scope of sliding area simulated by the numerical method are consistent with the automatic monitoring data that the potential sliding region is transfixion from the toe to the top of downstream face slope.

(5) Figure 10 shows the horizontal displacement of calculated and measured at the position of CX-01, and we can see that the value and regulation of them are consistent ultimately. The result indicates that the actual situation of the cofferdam engineering can be reflected excellently by the numerical simulation of Plaxis.

As shown in Figure 11 that the safety factors of cofferdam in each condition are reduced, the reduction rates are really small. It is because that the actual slope ratio of cofferdam is much more gentle than the design slope ratio and the permeability coefficient of filling materials is really
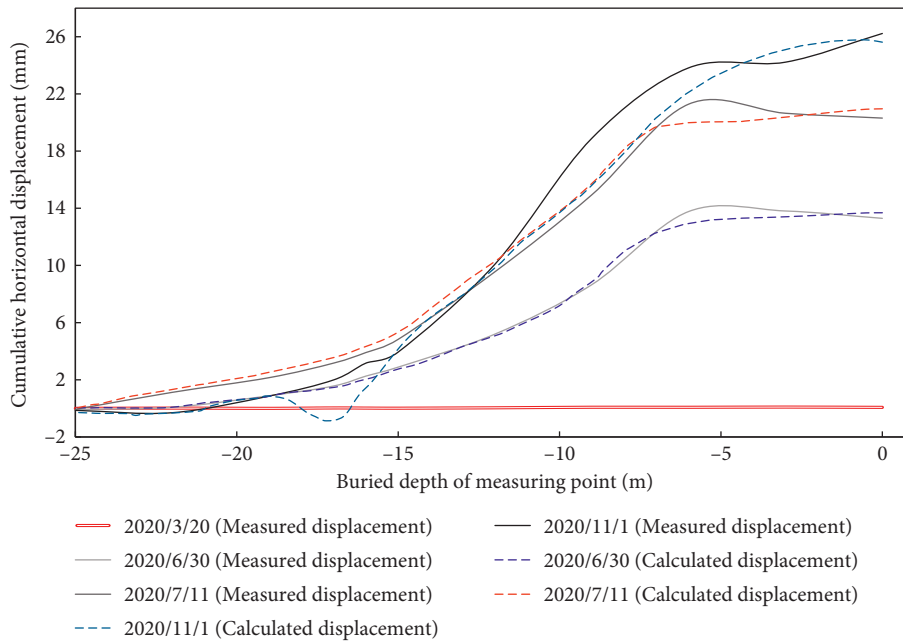
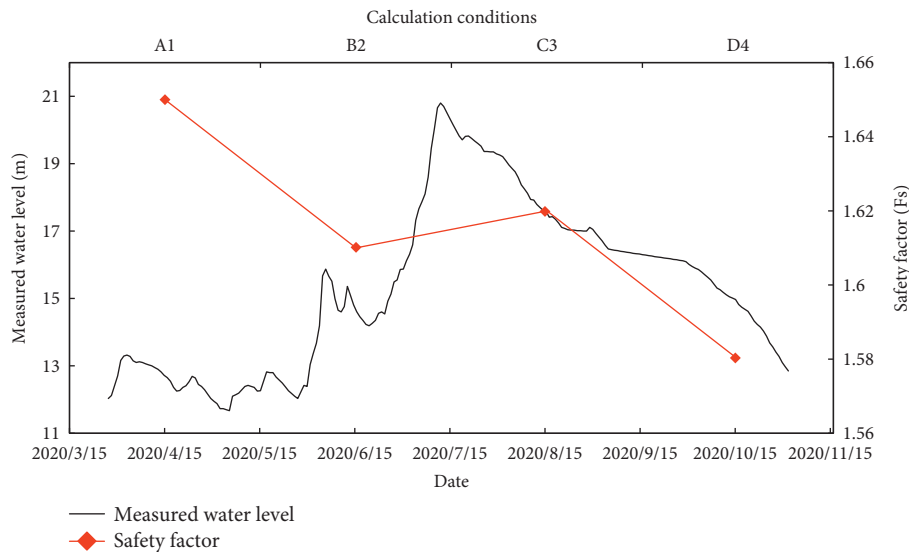FIGURE 10: Cofferdam slope soil horizontal displacement fitting curve.

FIGURE 11: Variation of safety factors under different operating conditions.

small so that the change of seepage pressure in the downstream face slope is tiny during the transient seepage state of high flood water level.

5. Conclusion

According to the results of field investigation, automatic monitoring, and numerical simulation analysis, the conclusion can be obtained as follows:

(1) The generation of tensile fissure on the top of cofferdam is closely related to the soil deformation of the downstream face slope. In addition, the rise of flood accelerates the growth of soil deformation rate

within 15 m below the cofferdam crest, which directly leads to the continuous development of fissure.

(2) According to the monitoring data, the water level variation inside the cofferdam is lagging to the rise of water level in flood season, and the high head difference between the flood level (20.78 m) and the cofferdam internal body water level (11 m) is an important reason for the local piping failure.

(3) For the throw filling soft clay cofferdam which is constructed in a gentle slope ratio type, the stability is controlled by the downstream face and the most dangerous situation is performed in the flood water decline process.

(4) The internal deformation of cofferdam can be reflected effectively by the real-time automatic monitoring method, and the early warning can be presented to ensure the stable operation of cofferdam.

Data Availability

The data are generated from experiments and can be available from the corresponding author upon request.

Conflicts of Interest

The authors declare that they have no conflicts of interest.

Acknowledgments

References

[1] X. Li, Z. Cao, and Y. Xu, "Characteristics and trends of coal mine safety development," *Energy Sources, Part A: Recovery, Utilization, and Environmental Effects*, vol. 12, pp. 1–19, 2020.

[2] S. Liu, X. Li, and D. Wang, "Investigations on the Mechanism of the Microstructural Evolution of Different Coal Ranks under Liquid Nitrogen Cold Soaking," *Energy Sources, Part A: Recovery, Utilization, and Environmental Effects*, vol. 7, pp. 1–17, 2020.

[3] X. L. Li, S. J. Chen, Q. M. Zhang, X. Gao, and F. Feng, "Research on theory, simulation and measurement of stress behavior under regenerated roof condition," *Geomechanics and Engineering*, vol. 26, no. 1, pp. 49–61, 2021a.

[4] X. L. Li, S. J. Chen, S. M. Liu, and Z. H. Li, "AE waveform characteristics of rock mass under uniaxial loading based on Hilbert-Huang transform," *Journal of Central South University*, vol. 28, no. 6, pp. 1843–1856, 2021b.

[5] X. L. Li, S. J. Chen, and S. Wang, "Study on in situ stress distribution law of the deep mine taking Linyi Mining area as an example," *Advances in Materials Science and Engineering*, vol. 9, no. 4, p. 5594181, 2021c.

[6] Yu Yang, G.-liang Feng, C.-jie Xu, B.-R. Chen, Da-X. Geng, and Bi-T. Zhu, "Quantitative Threshold of Energy Fractal Dimension for Immediate Rock-Burst Warning in Deep Tunnel: A Case Study," *Lithosphere*, vol. 2022, Article ID 1699273, 2022.

[7] F. Zhang, *Study on the Stability of Weir Slopes of High Soil and Rock Weirs with Deep Overburden*, China Three Gorges University, Yichang, China, 2015a.

[8] W. L. Shen, G. C. Shi, Y. G. Wang, J. B. Bai, R. F. Zhang, and X. Y. Wang, "Tomography of the dynamic stress coefficient for stress wave prediction in sedimentary rock layer under the mining additional stress," *International Journal of Mining Science and Technology*, vol. 31, pp. 653–663, 2021.

[9] X. G. Kong, D. He, X. F. Liu et al., "Strain characteristics and energy dissipation laws of gas-bearing coal during impact fracture process," *Energy*, vol. 242, Article ID 123028, 2022.

[10] X. G. Kong, S. G. Li, E. Y. Wang et al., "Experimental and numerical investigations on dynamic mechanical responses and failure process of gas-bearing coal under impact load," *Soil Dynamics and Earthquake Engineering*, vol. 142, Article ID 106579, 2021.

[11] Z. Li, X. Zhang, and Y. Wei, "Experimental study of electric potential response characteristics of different lithological samples subject to uniaxial loading," *Rock Mechanics and Rock Engineering*, vol. 54, pp. 397–408, 2021d.

[12] Y. Niu, E. Wang, and Z. Li, "Identification of coal and gas outburst-hazardous zones by electric potential inversion during mining process in deep coal seam," *Rock Mechanics and Rock Engineering*, vol. 2022, 2022.

[13] Y. Gao, Y. Yin, and B. Li, "Failure process simulation analysis of the Shenzhen "12.20" CDW landfill landslide: a case study," *Arabian Journal of Geosciences*, vol. 14, no. 12, pp. 1–12, 2021.

[14] Y. Gao, Y. Yin, and B. Li, "Investigation and dynamic analysis of the long runout catastrophic landslide at the Shenzhen landfill on December 20, 2015, in Guangdong, China," *Environmental Earth Sciences*, vol. 76, no. 1, pp. 1–16, 2017.

[15] T. Vitaly, N. Aleksandr, B. Vladimir, G. Inna, V. Yulia, and S. Olga, "Modeling of hydrophysical properties of the soil as capillary-porous media and improvement of mualem-van genuchten method as a part of foundation arrangement research," *Advances in Civil Engineering*, vol. 2016, Article ID 8176728, 7 pages, 2016.

[16] B. Wang, *The Influence of Water on the Management of Large Mounded Landslides*, Shijiazhuang Tiedao University, Shaoxing, China, 2014.

[17] C. Zhang, "Analysis of slope instability risk of high soil and rock but water cofferdams," *Chinese Journal of Rock Mechanics and Engineering*, vol. 34, no. S2, pp. 4157–4163, 2015b.

[18] H. Wu, G. Zhao, and S. Ma, "Failure behavior of horseshoe-shaped tunnel in hard rock under high stress: phenomenon and mechanisms," *Transactions of Nonferrous Metals Society of China*, vol. 32, no. 2, pp. 639–656, 2022a.

[19] G. Han, Yu Zhou, R. Liu, Q. Tang, X. Wang, and L. Song, "Infuence of surface roughness on shear behaviors of rock joints under constant normal load and stifness boundary conditions," *Natural Hazards*, vol. 2, pp. 1–18, 2022.

[20] Li Zhan, *Research on Multi-Conditions Test and Numerical Simulation Calculation of High Water Level Long-Term Inundation Embankment Project*, Heilongjiang University, Harbin, China, 2018.

[21] Y. Zhang, "Stability analysis of a typical landslide mass in the Three Gorges Reservoir under varying reservoir water levels," *Environmental Earth Sciences*, vol. 79, no. 1, pp. 243–254, 2020a.

[22] S. Luo, "Reactivation of a huge, deep-seated, ancient landslide: formation Mechanism, deformation characteristics, and stability," *Water*, vol. 12, no. 7, 2020.

[23] Z. Xiao, H. Deng, and J. Li, "Influence of intermittent decline in reservoir water level on the stability of mounded landslides," *Journal of Yangtze River Scientific Research Institute*, vol. 33, no. 8, pp. 114–119, 2016.

[24] Y. Wang, S. Kuang, and C. Yin, "Influence of flood level changes on shore beach stability," *Journal of Hydraulic Engineering*, vol. 46, no. 12, pp. 1398–1405, 2015.

[25] X. Wang, Y. Xiao, W. Shi et al., "Forensic Analysis and Numerical Simulation of a Catastrophic Landslide of

Dissolved and Fractured Rock Slope Subject to Underground Mining," *Landslides*, vol. 18, no. 5, 2022.

[26] J. B. Yan, Z. X. Zou, R. Mu et al., "Evaluating the stability of Outang landslide in the Three Gorges Reservoir area considering the mechanical behavior with large deformation of the slip zone," *Natural Hazards*, vol. 2022, 2022.

[27] Z. Li, J. Chen, and C. Tan, "Debris flow susceptibility assessment based on topo-hydrological factors at different unit scales: a case study of Mentougou district, Beijing," *Environmental Earth Sciences*, vol. 80, p. 365, 2021e.

[28] X. Zhang, W. Li, and B. Zeng, "Design and construction of double-wall steel cofferdam in deep water foundations. IOP Conference Series," *Earth and Environmental Science*, vol. 631, no. 1, Article ID 012054, 2021.

[29] F. Yuan and W. Chen, "Stability analysis of temporary cofferdam of a ship lock construction project in coastal area. IOP Conference Series," *Earth and Environmental Science*, vol. 768, no. 1, Article ID 012118, 2021.

[30] Z. Huang, S. Yang, N. Yang, M. Zhou, and A. Li, "Optimized design for large geotextile mats over soft soil," *Advances in Civil Engineering*, vol. 2021, no. 4, Article ID 4084961, 13 pages, 2021.

[31] H. Wu, M. A. Trigg, W. Murphy, and R. Fuentes, "A new global landslide dam database (raglad) and analysis utilizing auxiliary global fluvial datasets," *Landslides*, vol. 19, no. 3, pp. 555–572, 2022b.

[32] P. Amatya, D. Kirschbaum, and T. Stanley, "Rainfall-induced landslide inventories for lower mekong based on planet imagery and a semi-automatic mapping method," *Geoscience Data Journal*, pp. 1–13, 2022.

[33] S. Zhang and M. Hu, "Seepage and slope stability analysis of Kauswagan power station embankment in the Philippines during flooding," *Port and Waterway Engineering*, vol. 5, pp. 55–60, 2020b.

[34] Y. G. Zhang, J. Tang, Y. M. Cheng et al., "Prediction of landslide displacement with dynamic features using intelligent approaches," *International Journal of Mining Science and Technology*, vol. 2, no. 1, pp. 1–11, 2022.

[35] W. Zhong, J. Ouyang, D. Yang, X. Wang, Z. Guo, and K. Hu, "Effect of the in situ leaching solution of ion-absorbed rare earth on the mechanical behavior of basement rock," *Journal of Rock Mechanics and Geotechnical Engineering*, vol. 2, no. 1, pp. 39–51, 2022.

[36] X. Tang, Y. Zheng, and A. Wu, "Slope stability analysis under seepage action using PLAXIS finite element program," *Journal of Yangtze River Scientific Research Institute*, vol. 4, pp. 13–16, 2006.